Road Manhole Cover Delineation Using Mobile Laser Scanning Point Cloud Data

Yongtao Yu, *Member, IEEE*, Haiyan Guan, *Senior Member, IEEE*, Dilong Li, Chunhua Jin, Cheng Wang, *Senior Member, IEEE*, and Jonathan Li, *Senior Member, IEEE*

***Abstract*— Periodical road manhole cover measurement is extremely important to ensure road safety and reduce traffic disasters. This letter proposes an effective method for delineating road manhole covers from mobile laser scanning point cloud data. To improve processing efficiency, first, road surface points are segmented and rasterized into georeferenced intensity images. Then, object-oriented patches are generated through superpixel segmentation and further fed to a convolutional capsule network classifier for manhole cover detection. Finally, manhole covers are accurately delineated through a marked point process of disks. Quantitative evaluations on three data sets show that an average completeness, correctness, quality, and F_1-measure of 0.965, 0.961, 0.929, and 0.963, respectively, are obtained. Comparative studies with three existing methods confirm that the proposed method performs superiorly in delineating manhole covers of varying conditions and on complex road surface environments.**

***Index Terms*— Convolutional capsule network, manhole cover, marked point process, mobile laser scanning, point cloud.**

I. Introduction

MONITORING road surface conditions is greatly important for many transportation-related activities. The real-time and accurate information regarding road marks, road infrastructures, and road surface distresses can be used to regulate traffic flows, conduct driving behaviors, and avoid potential traffic accidents. Automated delineation of road surface fixtures is also a necessary input for many intelligent transportation systems, such as driver assistance and safety warning systems [1] and autonomous driving systems [2]. Therefore, to smooth transportation-related activities, to reduce serious casualties, and to improve road safety, periodical road asset surveys and road maintenance should be carried out.

Manuscript received January 16, 2019; revised April 13, 2019 and April 20, 2019; accepted May 6, 2019. This work was supported in part by the Natural Science Foundation of Jiangsu Province under Grant BK20160427, in part by the National Natural Science Foundation of China under Grant 61603146 and Grant 41671454, and in part by the Natural Science Research in Colleges and Universities of Jiangsu Province under Grant 16KJB520006. *(Corresponding author: Yongtao Yu.)*

Y. Yu and C. Jin are with the Faculty of Computer and Software Engineering, Huaiyin Institute of Technology, Huaian 223003, China (e-mail: allennessy.yu@gmail.com).

H. Guan is with the School of Remote Sensing and Geomatics Engineering, Nanjing University of Information Science and Technology, Nanjing 210044, China (e-mail: guanhy.nj@nuist.edu.cn).

D. Li is with the State Key Laboratory of Information Engineering in Surveying, Mapping, and Remote Sensing, Wuhan University, Wuhan 430072, China (e-mail: scholar.dll@gmail.com).

C. Wang and J. Li are with the Fujian Key Laboratory of Sensing and Computing for Smart Cities, School of Information Science and Engineering, Xiamen University, Xiamen 361005, China (e-mail: cwang@xmu.edu.cn; junli@xmu.edu.cn).

Color versions of one or more of the figures in this letter are available online at http://ieeexplore.ieee.org.

Digital Object Identifier 10.1109/LGRS.2019.2916156

As a common type of infrastructure on urban roads, road manholes are usually used to conduct rainwater, discharge sewage, bitt power, and telecommunication cables. Generally, for safety and beauty purposes, road manholes are covered with removable covers made of metals, concretes, or reinforced plastics. However, if the covers are stolen by thieves, broken by heavy trucks, or removed by workers, they form threatens to the moving vehicles and pedestrians and might cause severe traffic disasters and loss of life and property. Thus, timely and efficiently conducting manhole cover measurement is necessary for transportation management departments to perform road maintenance and repairs to ensure road safety, as well as for many intelligent transportation systems to recognize road distresses and direct driving behaviors.

Traditional means for road manhole cover measurements are usually carried out through onsite inspections of workers. Such methods are labor-intensive, time-consuming, and unsafe, especially on busy roads or in tunnels. Fortunately, due to the advances in optical imaging and data collection systems, collecting high-resolution road scene images can be rapidly and cost-effectively accomplished using mobile mapping systems or unmanned aerial vehicles. Consequently, manhole cover delineation using image processing techniques has been exploited in the literature. In [3], two methods were tested for detecting manhole covers. The first method adopted a geometrical filter to ascertain circular-shaped objects. The second method used a machine learning model to describe the texture features of manhole covers. In [4], the texture and intensity features of superpixels were computed and fed into a support vector machine classifier to detect candidate regions. The consistency and context of the candidate regions were analyzed using conditional random filed. A multiview manhole cover detection and localization method was proposed in [5]. In this method, manhole covers were first detected from single-view images through segmentation and filtering. Then, multiview processing was carried out to compute accurate locations of manhole covers. By combining improved Hough transform and image contrast, broken manhole covers were identified in [6]. In [7], a convolutional neural network was presented to detect and localize manhole covers. In addition, multisensor data fusion was also exploited for manhole cover detection [8].

Due to the advantages of mobile laser scanning systems in rapidly collecting real-world scale-invariant, 3-D, and rich-detailed road scene data with laser reflection properties, methods, and techniques based on the point cloud data have been developed for road scene object detection and

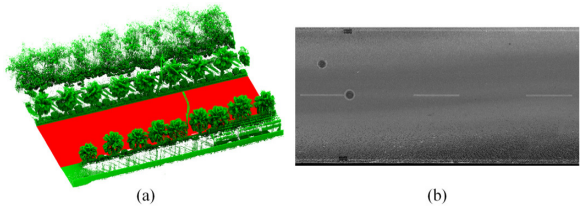

(a) (b)

Fig. 1. Illustrations of (a) segmented road surface points (red) and (b) generated georeferenced intensity image.

recognition [9], [10], such as road markings, vehicles, light poles, and traffic signs. Consequently, manhole cover detection has also been conducted using mobile laser scanning data. In [11], to facilitate data processing, road surface points were first segmented and interpolated into georeferenced feature images. Then, distance-dependent thresholding and multiscale tensor voting were applied to segment manhole cover candidates. Finally, manhole covers were detected using distance-based clustering and morphological techniques. A marked point process of disks was developed in [12] to detect circular-shaped manhole covers. In this method, manhole covers were modeled using marked points of disks and a Bayesian model. The marked point process was optimized based on the reversible jump Markov chain Monte Carlo algorithm. In [13], a multilayer feature generation model was constructed to depict high-order features of image patches. The detection of manhole covers was completed using a random forest model.

In this letter, we develop an effective method for delineating manhole covers from mobile laser scanning point cloud data. The proposed method performs superiorly in handling manhole covers of varying conditions and on different road surface environments. The contributions include: 1) a superpixel segmentation strategy for object-oriented patch generation; 2) a deep convolutional capsule network classifier with capsule convolution operations for manhole cover detection; and 3) a marked point process of disks for accurate manhole cover delineation.

II. Methodology

A. Road Segmentation and Intensity Image Generation

The collected mobile laser scanning data contain a large volume of 3-D points covering the entire road scene. In order to narrow the searching region and improve the efficiency, we only focus on the processing of road surface points. In this letter, we adopt the curb-line-based road segmentation method [14] to separate road surface points from the entire point cloud data. In this method, assisted by the vehicle trajectory, curb points are first located via profile analysis. Then, curb-lines fitted from the detected curb points are used to segment road surface points. The road surface segmentation result is illustrated in Fig. 1(a).

Instead of processing the discrete, unordered road surface points in 3-D space, we rasterize them into a 2-D georeferenced intensity image using the inverse distance weighted interpolation method [15]. In this method, first, road surface points are vertically partitioned into a series of grids with a specific spatial resolution (e.g., 2.5 cm). The spatial resolution is determined according to the point cloud density and the measurement accuracy tolerated. Then, the points within a grid are interpolated into a single pixel whose gray value is determined according to the distances to the grid center and intensities of these points. If a grid contains no points, the associated pixel value is set to be zero. The generated georeferenced intensity image is illustrated in Fig. 1(b).

B. Manhole Cover Detection

To accurately detect manhole covers from the intensity image, we construct a convolutional capsule network classifier. Different from conventional neural networks that consist of scalar neurons to encode the probabilities of the existence of specific features, a capsule network is composed of entity-oriented vectorial capsules. A capsule can be viewed as a vectorial combination of a set of neurons [16]. The instantiation parameters of a capsule represent a specific type of entity; the length of the capsule encodes the probability of the existence of that entity. Capsule networks have been proven to be more powerful and robust than conventional scalar neuron-based deep learning models in extracting intrinsic features [16]–[18]. Therefore, to obtain promising manhole cover detection performance, we extend the original capsule network to design a multilayer convolutional capsule network classifier.

Fig. 2 shows the complete architecture of our proposed convolutional capsule network classifier, which contains two conventional convolutional layers (Conv1 and Conv2), a primary capsule layer (PrimCap), two convolutional capsule layers (ConvCap1 and ConvCap2), and two fully connected capsule layers (FullCap1 and FullCap2). The two conventional convolutional layers function to extract low-level texture features from the input data. These features are further encoded into high-order capsules to represent different levels of entities. The Conv1 layer contains D_m feature maps, each of which is generated with a kernel size of $K_m \times K_m \times 1$. The Conv2 layer includes D_c feature maps, each of which is generated with a kernel size of $K_c \times K_c \times D_m$. For these two convolutional layers, we adopt the widely used ReLU as the activation function.

The PrimCap layer is a primary capsule layer that converts the scalar feature representations into the vectorial entity representations. The PrimCap layer is composed of D_p entity maps of S_p-dimensional capsules. It is constructed based on a conventional convolution operation on the Conv2 layer with a kernel size of $K_p \times K_p \times D_c$ and a feature map number of $D_p \times S_p$. After convolution operations, the generated feature maps are partitioned into groups to form D_p entity maps, each of which contains a set of capsules with a dimension of S_p. These capsules can not only estimate the probability of the existence of a specific entity through the vector length but also describe the attributes of that entity using the instantiation parameters.

The two convolutional capsule layers are used to extract high-order entity features from low-order entities encoded by capsules. This is carried out by performing capsule convolution operations and characterizing the extracted features using a new capsule. The ConvCap1 layer contains D_f entity maps of S_f-dimensional capsules generated with a kernel size of

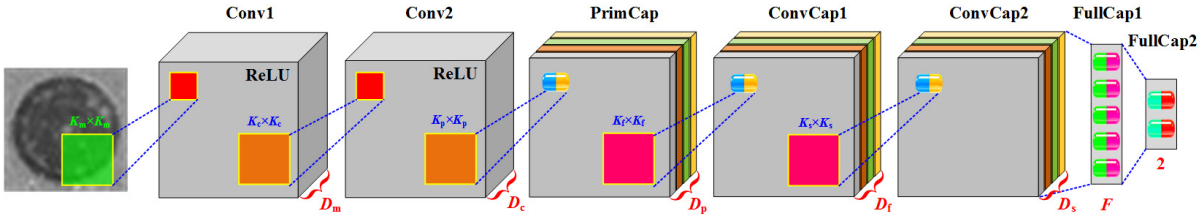

Fig. 2. Architecture of the convolutional capsule network classifier.

$K_f \times K_f \times D_p$. The ConvCap2 layer contains D_s entity maps of S_s-dimensional capsules generated with a kernel size of $K_s \times K_s \times D_f$. For the convolutional capsule layers, the total input to a capsule j is a weighted sum over all predictions from the capsules within the convolution kernel in the lower layer as follows:

$$\mathbf{C}_j = \sum_i a_{ij} \cdot \widehat{\mathbf{U}}_{j|i} \tag{1}$$

where C_j is the total input to capsule j; a_{ij} is the coupling coefficient indicating the degree of contribution that capsule i in the layer below activates capsule j; $\widehat{\mathbf{U}}_{j|i}$ is the prediction from capsule i to capsule j and it is calculated as follows:

$$\widehat{\mathbf{U}}_{j|i} = \mathbf{W}_{ij} \cdot \mathbf{U}_i \tag{2}$$

where U_i is the output of capsule i and $\mathbf{W}_{ij}$ is the network weight on the edge connecting capsules i and j. Specifically, the coupling coefficients between capsule i and all its connected capsules in the layer above sum to 1 and are determined by an iterative dynamic routing process [16]. Recall that we use the length of a capsule to evaluate the probability of the existence of an entity. Therefore, the nonlinear squashing function [16] is adopted as the activation function in the convolutional capsule layers to ensure that the shorter the capsules' lengths, the lower the probability estimations; whereas the longer the capsules' lengths, the higher the probability estimations. The squashing function is formulated as follows:

$$\mathbf{U}_j = \frac{\|\mathbf{C}_j\|^2}{1 + \|\mathbf{C}_j\|^2} \cdot \frac{\mathbf{C}_j}{\|\mathbf{C}_j\|}. \tag{3}$$

By such a conversion, short capsules are shrunk to almost zero length and long capsules approach to a length close to 1.

The two fully connected capsule layers combine all the capsules in the layer below to construct a high-level entity abstraction. The FullCap1 layer consists of F capsules, each of which has a dimension of S_m. The FullCap2 layer is a classification layer composed of two S_c-dimensional class-oriented capsules representing the manhole cover and the road surface, respectively. In these two layers, dynamic routing between capsules and the squashing function are also used to cast predictions and normalize the outputs of capsules.

The parameters of the convolutional capsule network classifier are iteratively adjusted through the error backpropagation process. In our implementation, the numbers of positive training samples of manhole covers and negative training samples of road surface are 2200, respectively. To effectively train the convolutional capsule network classifier toward classification tasks, we use the margin loss coupled with reconstruction regularization [16] as the objective function to direct the error backpropagation process.

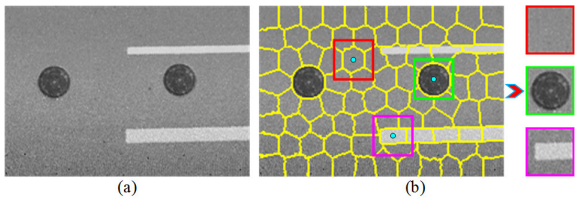

Fig. 3. Illustration of superpixel-based patch generation. (a) Road surface intensity image. (b) Superpixel segmentation result and generated patches.

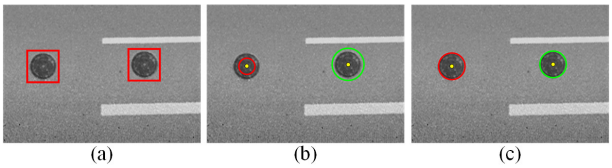

Fig. 4. Illustration of marked point process-based manhole cover delineation. (a) Detected manhole covers using the convolutional capsule network classifier. (b) Initial marked points. (c) Optimized marked points.

After the convolutional capsule network classifier is constructed, we apply it to the road surface intensity image to detect manhole covers. Instead of using the sliding window approach [13] to blindly move across the image, we propose a superpixel-based strategy to generate object-oriented meaningful and nonredundant patches. As shown in Fig. 3(b), first, the intensity image is segmented into a group of connected superpixels using the simple linear iterative clustering (SLIC) method [19]. Then, a square patch is generated centered at each superpixel. The generated patches are further input to the convolutional capsule network classifier to categorize them into manhole covers or the road surface. We use the length of the capsule in the FullCap2 layer to represent the certainty of a patch being an instance of a specific class. The class label of a patch is determined as follows:

$$L^* = \arg\max_k \|\mathbf{U}_k\| \tag{4}$$

where U_k is the output of a capsule in the FullCap2 layer. Fig. 4(a) illustrates the patches labeled as manhole covers.

C. Manhole Cover Delineation

To accurately delineate manhole covers and their locations, we adopt a marked point process [20]. In our implementation, a manhole cover is represented by a disk, which is modeled by a location coordinate and a radius. Let $\mathbf{X}$ be a marked point process of disks living in the following bounded space:

$$S = [x_{\min}, x_{\max}] \times [y_{\min}, y_{\max}] \times [r_{\min}, r_{\max}] \tag{5}$$

where $[x_{\min}, x_{\max}] \times [y_{\min}, y_{\max}]$ and $[r_{\min}, r_{\max}]$ correspond to the location space and the mark space, respectively. Then, the determination of the optimal set of marked points to delineate manhole covers in the intensity image is converted into the problem of minimizing the Gibbs energy function $U(\mathbf{X})$ composed of a data energy term and an interaction energy term

$$U(\mathbf{X}) = D(\mathbf{X}) + R(\mathbf{X}) \tag{6}$$

where $D(\mathbf{X})$ is the data energy term describing the consistency between the manhole covers and the intensity image; $R(\mathbf{X})$ denotes the interaction energy term indicating the locations of manhole covers without overlaps. The data energy term $D(\mathbf{X})$ is the accumulation of each individual energy associated with a marked point. The interaction energy term $R(\mathbf{X})$ considers pairwise interactions between two marked points. More details about the formulations of the Gibbs energy function and its two energy terms can be referred to [20].

Since the number of manhole covers and their potential regions have been detected using the convolutional capsule network classifier. Thus, we generate a set of marked points of disks centered at the patches labeled as manhole covers. As shown in Fig. 4(b), for a marked point, the location is initialized as the center of the corresponding patch; the radius is randomly initialized in the mark space $[r_{\min}, r_{\max}]$ following a uniform distribution. The adjustment and optimization of the parameters associated with each marked point are accomplished based on a simulated annealing assisted diffusion dynamic process [20]. After optimization, the location of each marked point is treated as the location of the associated manhole cover and the radius of the marked point indicates the size of the manhole cover. Fig. 4(c) illustrates the optimized marked points of disks delineating the tight contours and accurate locations of manhole covers.

III. Results and Discussion

A. Data Sets

The mobile laser scanning point cloud data used in this letter were acquired using the RIEGL VMX-450 mobile laser scanning system mounted on the roof of a Buick minivan driving at a speed of about 50 km/h on the urban roads in Xiamen, China. To evaluate the performance of our proposed manhole cover delineation method, we applied it to three selected mobile laser scanning point cloud data sets covering the road areas of Siming Road South (SRS), Software Park Phase II (SPP), and International Conference and Exhibition Center (ICEC). The remainder of the point cloud data was used to train the convolutional capsule network. The SRS data set covered an old four-lane asphalt-paved road segment of about 2998 m. The SPP data set covered a two-lane cement-paved road segment of about 3105 m. The ICEC data set covered a two-lane asphalt-paved road segment of about 2947 m. These three selected road sections covered typical urban roads paved with different materials (cement and asphalt) and with different geometric and road surface conditions (e.g., cracks).

B. Manhole Cover Detection and Delineation

To evaluate the manhole cover delineation performance, we applied our proposed method to the three point cloud data sets. Through computational and classification performance analysis, the parameters of the convolutional capsule network classifier were configured as in Table I. Table II details the manhole cover detection results achieved using the proposed method on the three data sets. In Table II, true positive (TP) and false positive (FP) denote the numbers of detected manhole covers and generated false alarms, respectively. As reflected in Table II, for each of the data sets, the majority of the manhole covers were correctly detected with quite a small proportion of false alarms. For visual inspections, Fig. 5 presents a subset of manhole cover delineation results. As shown in Fig. 5, benefiting from the development of the convolutional capsule network classifier and the marked point process of disks, the manhole covers of different conditions and on different road surface environments were effectively located and delineated. Specifically, the manhole covers partially painted by road markings and the manhole covers on crack-damaged roads were correctly detected and delineated. However, as shown by the manhole covers highlighted by blue circles in Fig. 5, these manhole covers exhibited extremely low contrast to the road surface and almost hided in the background. Caused by heavy traffic flows on this road segment and other natural factors, these manhole covers were covered with thick dusts and muds. Therefore, the proposed method failed to detect them. In addition, due to the high similarities of some road surface objects (e.g., large-area asphalt blocks) to manhole covers, these objects were falsely detected as manhole covers.

To quantitatively evaluate the manhole cover delineation results, the following four measures are adopted: *completeness* (*cpt*), *correctness* (*crt*), *quality* (*qat*), and F_1-*measure* (*fmr*) [13]. Table II details the quantitative

TABLE I
Parameter Setting of the Convolutional Capsule Network

Layer	Kernel Size	Map/Capsule No.	Capsule Dimension
Conv1	9×9×1	256	-
Conv2	5×5×256	256	-
PrimCap	3×3×256	128	16
ConvCap1	3×3×128	128	16
ConvCap2	3×3×128	128	16
FullCap1	-	64	16
FullCap2	-	2	16

TABLE II
Manhole Cover Detection Results and Quantitative Evaluations of Different Methods on the Three Test Data Sets

Method	Dataset	Ground Truth	Detection		Quantitative Evaluation			
			TP	FP	*cpt*	*crt*	*qat*	*fmr*
Proposed	SRS	165	160	7	0.970	0.958	0.930	0.964
	SPP	189	183	7	0.968	0.963	0.934	0.965
	ICEC	137	131	5	0.956	0.963	0.923	0.959
Method in [11]	SRS	165	123	21	0.745	0.854	0.661	0.796
	SPP	189	167	19	0.884	0.898	0.803	0.891
	ICEC	137	102	26	0.745	0.797	0.626	0.770
Method in [12]	SRS	165	146	16	0.885	0.901	0.807	0.893
	SPP	189	172	14	0.910	0.925	0.847	0.917
	ICEC	137	122	17	0.891	0.878	0.792	0.884
Method in [13]	SRS	165	158	7	0.958	0.958	0.919	0.958
	SPP	189	182	9	0.963	0.953	0.919	0.958
	ICEC	137	128	6	0.934	0.955	0.895	0.944

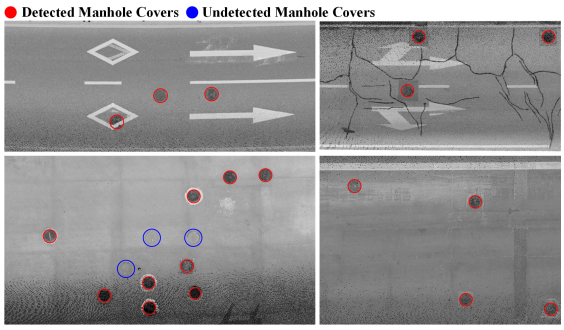

Fig. 5. Illustration of a subset of manhole cover delineation results.

evaluations on the three point cloud data sets. Specifically, the proposed method obtained an average completeness, correctness, quality, and F_1-measure of 0.965, 0.961, 0.929, and 0.963, respectively, in detecting manhole covers from the three data sets.

C. Comparative Study

To further evaluate the efficiency and accuracy of our proposed method in detecting manhole covers from mobile laser scanning data, we conducted a set of comparative studies with the following three methods: the tensor voting based method [11], the marked point process-based method [12], and the deep learning based method [13]. We applied these three methods to the three test data sets to perform manhole cover detection. Table II lists the manhole cover detection results and the quantitative evaluations. Among these three methods, the tensor voting-based method obtained a lower performance and generated more false alarms than the other two methods; whereas the deep learning based method achieved a promising and similar performance to our proposed method. In fact, depending on intensity thresholding and segmentation techniques, the tensor voting-based method lacked effective capabilities to handle manhole covers of varying conditions and on complex road surface environments. In contrast, the deep learning-based method exploited deep feature representations of manhole covers, thereby improving the detection performance. However, compared with the other two methods, the deep learning-based method cannot effectively delineate the shape and contour of a manhole cover. Comparatively, our proposed method was more robust and outperformed the other three methods in accurately detecting, locating, and delineating manhole covers from mobile laser scanning data.

IV. Conclusion

This letter has presented a complete workflow for delineating road manhole covers from mobile laser scanning data. Based on the superpixel-based patch generation strategy, the convolutional capsule network classifier, and the marked point process of disks, the proposed method performed effectively in delineating manhole covers of varying conditions and on complex road surface environments. Quantitative evaluations on three test data sets showed that the proposed method achieved an average completeness, correctness, quality, and F_1-measure of 0.965, 0.961, 0.929, and 0.963, respectively. Comparative studies with three existing methods demonstrated that the proposed method was more robust and outperformed the other three methods in accurately and correctly detecting, locating, and delineating manhole covers from mobile laser scanning point cloud data. However, the limitation of capsule networks is the relatively lower computational efficiency compared with the scalar neuron-based models. Our future work will explore radiometric calibration and fuse image data to further improve manhole cover delineation performance.

References

[1] H. Cheng, N. Zheng, X. Zhang, J. Qin, and H. V. D. Wetering, "Interactive road situation analysis for driver assistance and safety warning systems: Framework and algorithms," *IEEE Trans. Intell. Transp. Syst.*, vol. 8, no. 1, pp. 157–167, Mar. 2007.

[2] T. Li, M. Lee, C. Lin, G. Liou, and W. Chen, "Design of autonomous and manual driving system for 4WIS4WID vehicle," *IEEE Access*, vol. 4, pp. 2256–2271, 2016.

[3] J. Pasquet *et al.*, "Detection of manhole covers in high-resolution aerial images of urban areas by combining two methods," *IEEE J. Sel. Topics Appl. Earth Observ. Remote Sens.*, vol. 9, no. 5, pp. 1802–1807, May 2016.

[4] W. Sultani, S. Mokhtari, and H. B. Yun, "Automatic pavement object detection using superpixel segmentation combined with conditional random field," *IEEE Trans. Intell. Transp. Syst.*, vol. 19, no. 7, pp. 2076–2085, Jul. 2018.

[5] R. Timofte and L. van Gool, "Multi-view manhole detection, recognition, and 3D localisation," in *Proc. IEEE Int. Conf. Comput. Vis. Workshops*, Barcelona, Spain, Nov. 2011, pp. 188–195.

[6] F. Zhang, R. Chen, Y. Li, and X. Guo, "Detection of broken manhole cover using improved Hough and image contrast," *J. Southeast Univ.*, vol. 31, no. 4, pp. 553–558, Dec. 2015.

[7] B. Commandre, D. En-Nejjary, L. Pibre, M. Chaumont, C. Delenne, and N. Chahinian, "Manhole cover localization in aerial images with a deep learning approach," in *Proc. Int. Arch. Photogramm. Remote Sens. Spatial Inform. Sci.*, Hannover, Germany, vol. XLII-1/W1, pp. 333–338, May 2017.

[8] S. Ji, Y. Shi, and Z. Shi, "Manhole cover detection using vehicle-based multi-sensor data," in *Proc. Int. Arch. Photogramm. Remote Sens. Spatial Inform. Sci.*, Melbourne, Australia, vols. XXXIX–B3, pp. 281–284, May 2012.

[9] L. Ma, Y. Li, J. Li, C. Wang, R. Wang, and M. A. Chapman, "Mobile laser scanned point-clouds for road object detection and extraction: A review," *Remote Sens.*, vol. 10, no. 10, pp. 1531-1–1531-33, Sep. 2018.

[10] E. Che, J. Jung, and M. J. Olsen, "Object recognition, segmentation, and classification of mobile laser scanning point clouds: A state of the art review," *Sensers*, vol. 19, no. 4, pp. 810-1–810-42, Feb. 2019.

[11] H. Guan, Y. Yu, J. Li, P. Liu, H. Zhao, and C. Wang, "Automated extraction of manhole covers using mobile LiDAR data," *Remote Sens. Lett.*, vol. 5, no. 12, pp. 1042–1050, Nov. 2014.

[12] Y. Yu, J. Li, H. Guan, C. Wang, and J. Yu, "Automated detection of road manhole and sewer well covers from mobile LiDAR point clouds," *IEEE Geosci. Remote Sens. Lett.*, vol. 11, no. 9, pp. 1549–1553, Sep. 2014.

[13] Y. Yu, H. Guan, and Z. Ji, "Automated detection of urban road manhole covers using mobile laser scanning data," *IEEE Trans. Intell. Transp. Syst.*, vol. 16, no. 6, pp. 3258–3269, Dec. 2015.

[14] Y. Yu, J. Li, H. Guan, C. Wang, and J. Yu, "Semiautomated extraction of street light poles from mobile LiDAR point-clouds," *IEEE Trans. Geosci. Remote Sens.*, vol. 53, no. 3, pp. 1374–1386, Mar. 2015.

[15] H. Guan, J. Li, Y. Yu, C. Wang, M. Chapman, and B. Yang, "Using mobile laser scanning data for automated extraction of road markings," *ISPRS J. Photogramm. Remote Sens.*, vol. 87, pp. 93–107, Jan. 2014.

[16] S. Sabour, N. Frosst, and G. Hinton, "Dynamic routing between capsules," in *Proc. Adv. Neural Inf. Process. Syst.*, 2017, pp. 1–11.

[17] G. Hinton, S. Sabour, and N. Frosst, "Matrix capsules with EM routing," in *Proc. Int. Conf. Learn. Rep.*, Vancouver, Canada, May 2018, pp. 1–15.

[18] N. Frosst, S. Sabour, and G. Hinton, "DARCCC: Detecting adversaries by reconstruction from class conditional capsules," in *Proc. Neural Inform. Process. Syst. Workshop Secur. Mach. Learn.*, 2018, pp. 1–13.

[19] R. Achanta, A. Shaji, K. Smith, A. Lucchi, P. Fua, and S. Süsstrunk, "SLIC superpixels compared to state-of-the-art superpixel methods," *IEEE Trans. Pattern Anal. Mach. Intell.*, vol. 34, no. 11, pp. 2274–2282, Nov. 2012.

[20] F. Lafarge, G. Gimel'farb, and X. Descombes, "Geometric feature extraction by a multimarked point process," *IEEE Trans. Pattern Anal. Mach. Intell.*, vol. 32, no. 9, pp. 1597–1609, Sep. 2010.